

Available online at [www.sciencedirect.com](http://www.sciencedirect.com)

SCIENCE @ DIRECT®

Vision Research 44 (2004) 2587–2596

---



---

**Vision  
Research**


---



---

[www.elsevier.com/locate/visres](http://www.elsevier.com/locate/visres)

# Backward masking and the central performance drop

Rick Gurnsey<sup>\*</sup>, David Di Lenardo, Cindy Potechin

*Department of Psychology, Concordia University, 7141 Sherbrooke Street West, Montréal, Qué., Canada H4B 1R6*

Received 8 September 2003; received in revised form 18 May 2004

---

## Abstract

Kehrer [Spatial Vision 2 (1987) 247] found that texture discrimination performance sometimes peaks in the parafovea rather than at the fovea, and he referred to this phenomenon as the central performance drop (CPD). Kehrer used a backward mask to limit performance and Morikawa [Vision Res. 40 (2000) 3517] argued that in some cases the temporal aspects of the backward mask may be critical to the emergence of the CPD. In one experiment Morikawa showed that the CPD does not emerge when a simultaneous noise-mask (different from the mask used by Kehrer) is used to limit performance. In another experiment Morikawa showed that unmasked texture displays comprising short lines do not elicit the CPD. In both cases, changes in the temporal aspects of the texture displays were accompanied by changes in the spatial structure of the mask or stimulus. For the *spatio-temporal* theory of the CPD to be sustained one would have to show that noise masks elicit a CPD when used as backward masks and that the short-line textures elicit a CPD when followed by backward masks. Our evidence provides little if any support for either of these predictions. Furthermore, an analysis of a simple filter-rectify-filter model of texture segmentation shows that a greatly attenuated CPD is to be expected when a noise mask is used as a source of spatial noise.

© 2004 Elsevier Ltd. All rights reserved.

*Keywords:* Texture; Peripheral vision; Backward masking; Central performance drop

---

## 1. Introduction

Performance in spatial vision tasks typically declines as stimuli of fixed size are moved from fovea to the periphery. In fact, there is a substantial literature devoted to characterizing eccentricity dependent sensitivity losses, and the stimulus magnifications needed to offset these losses (e.g., Poirier & Gurnsey, 2002; Wilson, Levi, Maffei, Rovamo, & De Valois, 1990). In striking contrast to the usual effects of eccentricity on spatial discriminations, Kehrer (1987) found that detection of a texture comprising oblique lines of a particular orientation embedded in a larger background of orthogonally oriented lines *improves* as the target texture is moved away from the fovea. Kehrer coined the term “central per-

formance drop” (CPD) to denote the sub-optimal detection performance at foveal or near-foveal locations. This basic result has been found in a number of labs and in a variety of tasks (Gurnsey, Pearson, & Day, 1996; Joffe & Scialfa, 1995; Kehrer, 1987, 1989, 1997; Meinecke, 1989; Meinecke & Donk, 2002; Meinecke & Kehrer, 1994; Yeshurun & Carrasco, 1998, 2000) and has been established as a reliable phenomenon. The question is: Why does the CPD occur?

In Kehrer’s (1989) task a disparate texture region ( $\approx 1.75^\circ$  high and wide) was embedded in a background texture that was  $24^\circ$  wide and  $3.1^\circ$  high. Textures comprised left or right oblique line segments and lines in the disparate texture differed from those in the background texture by  $90^\circ$ . On each trial the disparate texture was either present or absent and, when present, could appear at one of 47 positions along the horizontal midline of the display. Hit rate was the dependent measure. In such a task it might be argued that the CPD

---

<sup>\*</sup> Corresponding author. Tel.: +1-514-848-2243; fax: +1-514-848-4545.

*E-mail address:* [rick.gurnsey@concordia.ca](mailto:rick.gurnsey@concordia.ca) (R. Gurnsey).

arises because participants are more conservative in their responses for stimuli presented near the fovea. This explanation can be rejected for three reasons: First, [Kehrer \(1989\)](#) had participants indicate where they thought the target had been each time they made a false alarm. It was found that participants were more likely to identify foveal regions on these trials. This is exactly contrary to what one would expect based on a criterion shift explanation. Second, in a task similar to that of [Kehrer \(1987\)](#), [Gurnsey et al. \(1996\)](#) measured  $d'$  for texture discrimination at a range of eccentricities. It was found that  $d'$  was maximal at 3°–4° from fixation and dropped as the texture region was moved closer to fixation or further into the periphery. Finally, [Morikawa \(2000\)](#) and [Potechin and Gurnsey \(2003\)](#) used a four alternative forced choice task (4AFC) to assess sensitivity to texture differences. As in [Kehrer's \(1987\)](#) study, the foreground and background textures were left and right oblique line segments. The disparate region could appear at one of eight eccentricities (distances from fixation) along one of the four diagonal meridians. The participant's task was to identify the quadrant containing the disparate region. In this task there is no issue of setting a criterion and yet very pronounced CPDs were obtained in both studies. Therefore, an eccentricity dependent criterion shift may be rejected as the source of the CPD.

In many studies of the CPD texture displays have been followed by a mask to avoid ceiling effects that would otherwise occur. This methodological feature has led to a spatio-temporal account of the CPD. [Kehrer \(1989\)](#) argued that low frequencies are processed faster than high frequencies, and that foveal processing is more associated with high frequencies and peripheral vision more associated with low frequencies. These assumptions together suggest that "processing speed" increases from with distance from the fovea. On this view, a texture boundary presented at the fovea is segmented on the basis of high-frequency information. A mask presented at a stimulus onset asynchrony (SOA) of 50 ms (for example) could interfere with the segmentation process. However, segmentation based on lower frequencies available in the periphery might be completed prior to the onset of the mask. The existence of the CPD leads to the further assumption that low frequencies are not processed as effectively in the fovea as in the periphery. Therefore, [Kehrer](#) posited an association between the frequency selectivity of spatial filters, their sensitivity at different eccentricities and their speed of operation.

This spatio-temporal theory is supported by the finding that the performance peak moves further into the periphery as the fundamental frequency of the texture decreases, and that performance improves as the interval between stimulus and mask increases ([Gurnsey et al., 1996](#); [Joffe & Scialfa, 1995](#); [Kehrer, 1989](#)). However,

even though the performance peak moves to greater eccentricities as inter-element spacing increases, the absolute level of performance also drops ([Gurnsey et al., 1996](#); [Kehrer, 1989](#)). This seems inconsistent with the processing speed aspect of [Kehrer's \(1989\)](#) original suggestion. Furthermore, it has been shown that a backward mask is not required for the CPD to occur ([Morikawa, 2000, Expt. 4](#); [Potechin & Gurnsey, 2003](#); [Yeshurun & Carrasco, 2000](#)).

[Gurnsey et al. \(1996\)](#) argued that the CPD could be understood in strictly spatial terms. They suggested that the sizes of filters (e.g., Gabor filters) involved in texture segmentation vary as a function of eccentricity; specifically, textures are segmented based on the responses of small filters at the fovea and large filters in the periphery. In addition [Gurnsey et al. \(1996\)](#) suggested that the region over which textures are compared is tied to the size of the filters involved; viz, at the fovea smaller regions are compared than in the periphery. A consequence of this organization is that optimal performance will occur when the scale of the texture (i.e., inter-element spacing) is matched to the scale of the available segmentation mechanism. At the fovea the segmentation mechanisms may be too small relative to the textures, whereas in the far periphery they are too large. At some intermediate eccentricity the texture and the mechanism are optimally matched thus yielding a performance peak.

Most empirical data are consistent with the spatial account ([Gurnsey et al., 1996](#); [Joffe & Scialfa, 1995](#); [Kehrer, 1987, 1989, 1997](#); [Yeshurun & Carrasco, 1998](#)) and the assumptions of the spatial theory can be used to model data from several experiments showing the CPD ([Gurnsey & Poirier, 2003](#); [Kehrer, 1997](#); [Kehrer & Meinecke, 2003](#); [von Berg, Ziebell, & Stiehl, 2002](#)). Finally, as noted, [Morikawa \(2000\)](#) and [Potechin and Gurnsey \(2003\)](#) showed that a backward mask is not necessary in order to obtain a CPD.

[Morikawa \(2000\)](#) presented results that might be seen as more consistent with a temporal account than a spatial account of the CPD. [Morikawa](#) used a four alternative forced choice (4AFC) task in which participants identified the quadrant containing a disparate texture (left and right obliques as in the top left panel of [Fig. 1](#)). When performance was limited by a backward mask there was a clear CPD. However, when a *simultaneous noise mask* (comprising single pixel dots having a density of 6–7%) was used to limit performance no CPD was obtained; performance was flat from fixation to the near periphery and then dropped monotonically at even further eccentricities. As well, when performance was limited without a backward mask by reducing the length of the lines comprising the textures, no CPD was obtained. One interpretation of these data is that the backward mask used in the classic experiments of [Kehrer \(1987, 1989\)](#) did not function simply as a source of spa-

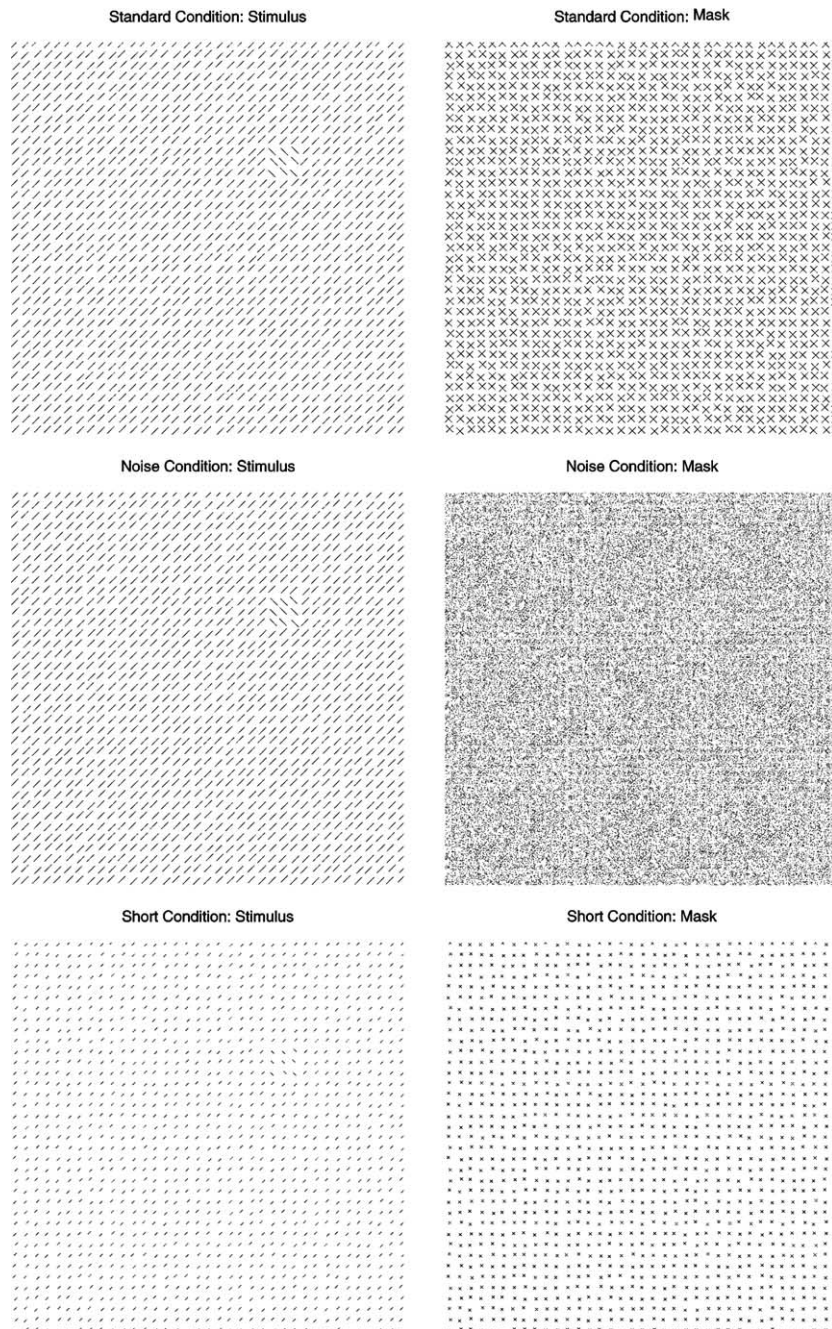


Fig. 1. Examples of the stimuli used in the three conditions of the experiment.

tial noise as was argued by Potechin and Gurnsey (2003). Rather, it might be argued that the temporal relationship between stimulus and mask was essential for the emergence of the CPD. However, this interpretation is limited on both theoretical and empirical grounds.

First, theoretically, it is not obvious that a failure to find a CPD with a simultaneous noise mask is inconsistent with standard spatial models of the CPD (e.g., Gurnsey et al., 1996; Kehrer, 1997; Kehrer & Meinecke, 2003). In Section 4 we present a simple filter–rectify–fil-

ter (FRF) model of texture segmentation and demonstrate that its response to a texture boundary in the presence of an X-type mask (e.g., Fig. 1, top right) is quite different than its response to the same texture boundaries in the presence of a noise mask (e.g., Fig. 1, centre right). In fact this difference roughly parallels the results of Morikawa (2000).

Second, to test the importance of the backward mask in the CPD experimentally, Morikawa (2000) changed two aspects of the displays in each of the experiments described above. In one case the mask was changed

from X-type patterns (Fig. 1, top right) to random dots (Fig. 1, middle row, right) and, the mask was changed from a backward mask to a simultaneous mask. Failure to find the CPD could be attributable to the change in the spatial structure of the mask or the temporal relationship between the stimulus and mask. In the second case, the stimulus lines were shortened and the backward mask was eliminated. Again, the failure to find a CPD could be attributed to either of these changes. For the temporal theory to be sustained, one would have to show that noise masks produce a CPD when used as backward masks but not when used as simultaneous masks. Furthermore, for the short-line experiment to prove the involvement of the temporal aspects of a backward mask in the CPD, one would have to show that a CPD occurs for the short-line textures when a backward mask is used. The following experiments were designed to assess the importance of the temporal aspects of backward masks to the CPD.

## 2. Method

### 2.1. Participants

The participants were 35 students (10 males and 25 females) recruited from undergraduate psychology classes at Concordia University. All the participants reported normal or corrected to normal vision and wore their refractive correction during testing. All participants were naive psychophysical observers and had a mean age of 23.5 years. One participant was excluded from the analysis because she misunderstood the task instructions.

### 2.2. Apparatus

Stimulus presentation and data collection were controlled by a Macintosh G4 computer attached to an Apple 21-in. multiscan, colour monitor. The monitor had a frame rate of 85 Hz, and a screen resolution of 1280×1024 pixels; pixel width was 0.28 mm. Participants viewed the monitor from approximately 69 cm and a chinrest was used to stabilize head position. The experiment was conducted in a windowless room and indirect illumination was provided by a shielded 60-W lamp placed to one side of the computer monitor.

### 2.3. Stimuli

Fig. 1 provides illustrations of the stimuli and masks used in the experiment. The lines and dots in Fig. 1 are black on white for purposes of illustration only. In the actual experiments they were white (69 cd/m<sup>2</sup>) on black (0.1 cd/m<sup>2</sup>) as in the experiments of Morikawa (2000).

Three different conditions were tested, each employing stimuli and masks that closely matched those used by Morikawa (2000). The first condition employed a left and right oblique line-elements stimulus (Fig. 1, top left) and a backward-mask (Fig. 1, top right). We refer to this as the *standard condition*. Each micropattern was drawn within a 28×28 pixel grid, and each left and right oblique line was 18 pixels in length along a diagonal direction. The position of each line was randomly jittered by +2 pixels from the centre of the grid. The mask element associated with each texture element combined the texture element and its reflection, making X-like patterns.

The second condition employed the same texture stimulus as in the standard condition (Fig. 1, middle left) and a noise mask (Fig. 1, middle right). This noise mask had 6% density of white dots on a black background and is identical to the simultaneous noise mask used by Morikawa (2000). We refer to this as the *noise condition*. The third condition was identical to the standard condition in all respects except that the lines comprising the texture and mask were 40% of the length of those in the standard condition (i.e., 7 pixels). We refer to this as the *short condition*.

All stimulus displays comprised 36 rows and 46 columns of micropatterns. When viewed from 69 cm these displays subtended 23.1° vertical and 29.3°. A 3×3 region was embedded in this larger background texture. The orientation of the lines in the disparate region was 90° different from those in the background. This foreground region was presented at eight eccentricities (1.39°, 2.32°, 3.25°, 5.11°, 6.97°, 8.82°, 10.68°, and 12.54°) per quadrant along the two diagonal axes (i.e., 45° from vertical) that intersect the center of the display. The orientations of both the target and background elements were randomly varied between trials and balanced within each condition so that the absolute orientation of the elements would not facilitate texture segregation performance.

### 2.4. Procedure

Each experimental trial consisted of the sequential presentation of a fixation dot, stimulus, backward-mask, and response screen. The fixation stimulus was a 5×5 pixel, blue dot presented at the centre of the screen for 400 ms prior to the onset of the stimulus display and remained on through the presentation of the stimulus and the mask. The stimulus was presented for durations of 11.8, 23.5, 35.3 and 47.1 ms, which corresponded to 1–4 frame refreshes, respectively. Each stimulus was followed by a mask on the subsequent frame; the mask remained on the screen for 300 ms. The SOAs used were the shortest possible and covered performance from floor to ceiling in pilot studies. Following the offset of the mask the fixation dot changed to red and remained

red until participants made a valid response. The task was to indicate which quadrant contained the disparate region. Participants indicated their choices by pressing preselected keys on the keyboard.

There were 256 trials in each block of the experiment;  $8(\text{eccentricities}) \times 4(\text{SOAs}) \times 4(\text{quadrants}) \times 2(\text{replications}) = 256$  trials per block. There were three replications of each block for a total of  $3 \times 256 = 768$  trials per experimental session. Participants were encouraged to take breaks if necessary.

Prior to the experimental session, participants were presented with 40 practice trials. During the practice period, stimuli were presented once at each eccentricity (in a randomly chosen quadrant) at SOAs of 941.2, 470.6, 117.6, 58.8, and 23.5 ms. The trials proceeded in a fixed sequence from the longest SOAs to the shortest SOAs so that discrimination would be initially easy and become increasingly difficult, eventually reaching the level of difficulty in the experimental trials.

Participants were assigned randomly to one of the three experimental conditions (standard, noise or short). There were 11 participants in the standard and short-line conditions, and 12 participants in the noise-mask condition.

### 3. Results

For each of the the 4 (SOAs)  $\times$  8 (eccentricities) = 32 cells within each condition 24 responses were collected. The dependent measure was the proportion of correct responses in each cell. For each condition, the data were submitted to a  $4 \times 8$  within-subjects ANOVA. All statistically significant results were corrected with the Greenhouse–Geisser correction procedure.

#### 3.1. The standard condition

The results of the standard condition are summarized in the left panel of Fig. 2. There was a main effect of duration [ $F(3,30) = 120, p < 0.0001$ ], and of eccentricity

[ $F(7,70) = 25.4, p < 0.0001$ ]. These results indicate that performance improves with increases in SOA and vary as a function of eccentricity. There was also a statistically significant interaction of SOA and eccentricity [ $F(21,210) = 3.35, p < 0.0001$ ].

The principal objective of the study was to assess the CPD in each of the three conditions. We did this by assessing the linear trend in the five eccentricities closest to fixation (i.e., 1.39°, 2.32°, 3.25°, 5.11° and 6.97°) for each of the four SOAs. The furthest eccentricity tested (6.97°) represented the performance peak at the shortest SOA in the standard condition (Fig. 2, left panel). The analyses revealed statistically significant linear trends at all SOAs [ $F(1,10) = 67.1, 37.2, 17.5$  and  $11.3$  for SOAs of 11.8, 23.5, 35.3 and 47.1 ms, respectively; all  $p < 0.01$ ]; i.e., there was a statistically significant CPD at all SOAs. We repeated this analysis for eccentricities 2.32°–6.97°; i.e., we eliminated the location nearest fixation for reasons to be discussed later. (These points are printed in light grey in Fig. 2.) For SOAs of 11.8, 23.5 and 35.3 the trends remained statistically significant [ $F(1,10) = 29.8, 15.5$  and  $7.32$ , respectively, all  $p < 0.05$ ] and for SOA = 47.1 the trend approached significance [ $F(1,10) = 3.42, p < 0.09$ ].

#### 3.2. The noise condition

The results of the noise condition are summarized in the centre panel of Fig. 2. There was a statistically significant effect of SOA [ $F(3,33) = 143, p < 0.0001$ ] and of eccentricity [ $F(7,77) = 13.5, p < 0.0001$ ]. These results indicate that performance improves with increases in SOA and vary significantly as a function of eccentricity. There was also a statistically significant interaction of SOA and eccentricity [ $F(21,231) = 5.48, p < 0.0001$ ].

The linear trend analysis for the first five eccentricities were statistically significant for SOAs 23.5, 35.3 and 47.1 [ $F(1,11) = 13.8, 5.53$  and  $8.12$ , respectively; all  $p < 0.05$ ] but not for SOA = 11.8. An examination of the centre panel of Fig. 2 suggests that the linear trend is attributable to a drop in performance at the position nearest to

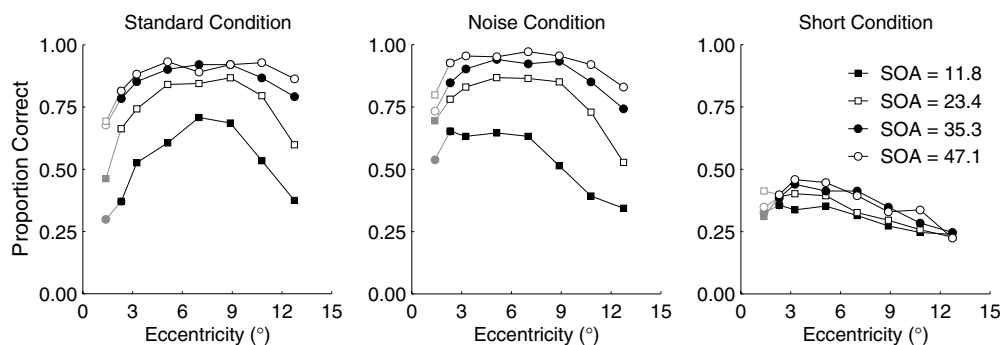


Fig. 2. Average proportion of correct responses as a function of eccentricity for the standard ( $n = 11$ ), noise-mask ( $n = 12$ ) and short line ( $n = 11$ ) conditions.

fixation. When the trend analyses were rerun for the four eccentricities from 2.32° to 6.97°, no statistically significant linear trends were found. This contrasts with the corresponding analyses of the standard condition in which the CPD remained statistically significant at three of four SOAs when the point nearest to fixation was dropped from the analysis.

### 3.3. The short condition

The results of the short condition are summarized in the right panel of Fig. 2. The ANOVA revealed statistically significant effects of SOA [ $F(3,30)=4.87$ ,  $p<0.01$ ] and eccentricity [ $F(7,70)=4.53$ ,  $p<0.001$ ], indicating that performance improved with SOA but decreased with eccentricity; i.e., there is no evidence of a CPD. There was no statistically significant interaction between SOA and eccentricity. It may be that no CPD was found in this condition because of a floor effect and that if longer SOAs had been used a CPD might have emerged. On the other hand, we show in Section 4 that failure to find a CPD in the Short condition is consistent with at least one version of a standard, FRF texture segmentation mechanism.

### 3.4. Comparison with Morikawa (2000)

Some of the present results show a marked similarity to those of Morikawa (2000). Fig. 3, left shows the data from the three conditions of Morikawa's (2000) experiment. Fig. 3, right shows data from the shortest SOA in the standard and noise conditions, and data from the longest SOA of the short-line condition.<sup>1</sup> of the present experiments. There is a clear similarity in the pattern of results in the two panels. These data clearly show that using noise as a backward mask, or masking the short-lines does not inevitably lead to a CPD. Rather, these data seem more consistent with the idea that differences in the spatial structure of the noise mask (vs. the X-mask) eliminate the CPD in the noise condition. In the case of the short-line condition it seems that reducing the length of the lines in itself is sufficient to eliminate the CPD.

The data from other SOAs complicate this simple picture slightly. The data in Fig. 2 have been replotted in Fig. 4 to show how the three conditions compare at each of the four SOAs. The pattern of results is similar across all SOAs. The standard condition always produces the largest drop in performance at fixation relative to peak performance in the periphery. Except at the shortest SOA, the noise condition yields a modest CPD. (We noted earlier that the modest CPD in the

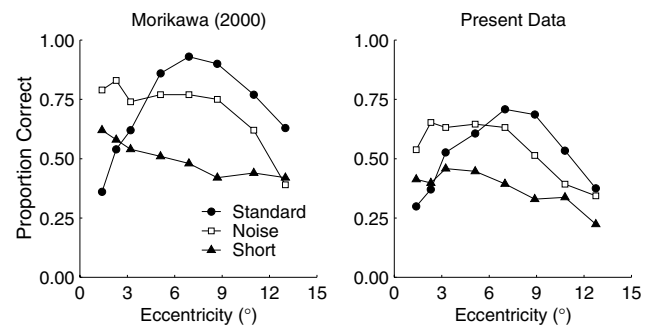


Fig. 3. Comparison with the results of Morikawa (2000); see text for details.

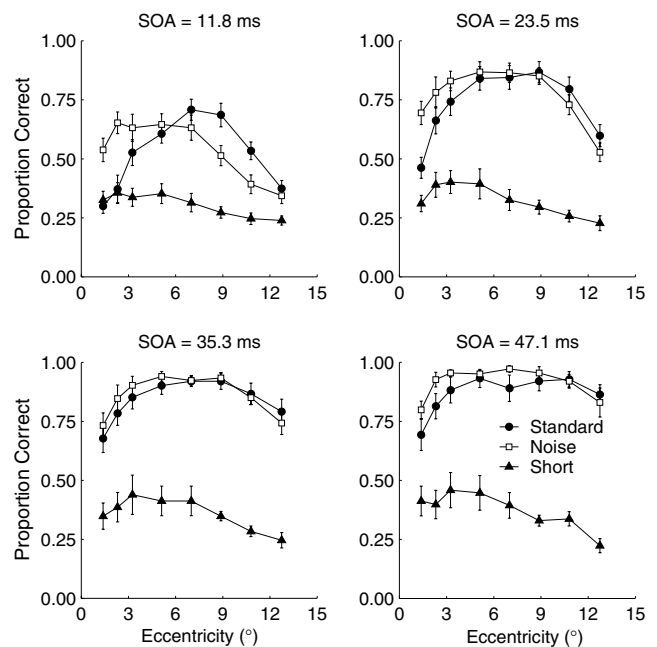


Fig. 4. Each panel shows the condition by eccentricity interaction for a different SOA. Error bars are  $\pm$ SEM.

noise condition is heavily influenced by the position nearest fixation and may reflect positional uncertainty rather than a true CPD.) It could be argued, perhaps, that the modest CPDs in the noise conditions at longer SOAs are evidence that temporal factors produce the CPD. A counter-argument might be that the noise and X-masks have different effects across eccentricities; e.g., relative to the standard X-mask, the noise mask is less effective near fixation and more effective in the periphery. But, this counter-argument raises the obvious question: exactly what does the spatial model predict the effects of these manipulations should be? To address this question we constructed a model of texture discrimination that instantiates the spatial account and compared its responses to those of psychophysical observers.

<sup>1</sup> The longest SOA was used because the data in this condition were the furthest from the floor.

## 4. Analysis

### 4.1. An FRF model of texture segmentation

The model we constructed combined the responses of two simple FRF texture segmentation mechanisms (e.g., Gurnsey & Browse, 1989) that were identical in all respects except the orientation selectivity of the initial filters. These first layer filters were formed from the difference of three offset Gaussians (DOOGs) as described by Young (1985) and Malik and Perona (1990). The spread of each Gaussian along its major axis was three times that of the spread along its minor axis ( $\sigma_f$ ). The flanking Gaussians were displaced by  $\pm\sigma_f$  units from the central Gaussian in a direction parallel to the minor axis. The three Gaussians were combined linearly as a weighted sum with weights  $-1, 2, -1$ . The resulting filters were oriented  $\pm 45^\circ$  from vertical and hence selective for left and right oblique lines. The second stage filters were circularly symmetric, difference-of-Gaussians (DOGs). The spread ( $\sigma_{se}$ ) of the excitatory Gaussian was  $3\sigma_f$  and that of the inhibitory Gaussian ( $\sigma_{si}$ ) was  $1.6\sigma_{se}$  (Kehrer, 1997). The spatial theory of the CPD holds that mechanisms of this sort exist at each eccentricity and differ only in spatial scale. The scale of the mechanism just described is determined by the single parameter  $\sigma_f$ . Therefore, different eccentricities may be simulated by varying  $\sigma_f$ .

The model was applied to samples from the textures shown in Fig. 1 (left panels) scaled to 50% of their original size. Each texture patch comprised 64 oriented lines (an  $8 \times 8$  region). Except for the display sizes and scaling, the textures were exactly as described in Section 2. Target-present (signal) displays contained a  $3 \times 3$  sub-region of lines oriented  $-45^\circ$  and the remaining lines were oriented  $45^\circ$ . All lines in the target-absent (null) displays were oriented  $45^\circ$ . Masks were also created as described in Section 2 and added to the stimuli. Adding stimulus and mask was intended to model the effect of mask delay in the experiments; i.e., increasing the weight given to the stimulus models increases in SOA. Each stimulus (either a signal stimulus or a null stimulus) was, therefore, a weighted sum of the texture display and the mask; i.e., stimulus =  $\alpha I + M$  for  $\alpha = 0.80, 1.09, 1.47, \text{ and } 2.00$ , where  $I$  could be a signal or null display and  $M$  could be a noise or X-type mask.

The model response ( $R$ ) combined the outputs of the two parallel FRF streams. In each stream the stimulus was convolved with the DOOG (oriented  $\pm 45^\circ$ ) and the result half-wave rectified. The rectified signal was then convolved with the DOG and the results squared, producing  $R_{45}$  and  $R_{-45}$ . The model output was the square root of the sum of the responses in the two streams (i.e.,  $R = \sqrt{R_{45} + R_{-45}}$ ). Such models are designed to respond well to texture discontinuities (Gurn-

sey & Browse, 1989) and thus the maximum model response should be greater when a texture discontinuity is present than when it is not. Therefore, we used the mean of the largest 25% of second layer responses as our measure of response magnitude. These responses were computed within a circular region that enclosed the disparate region in the signal display and an equivalent region in the target absent display.

### 4.2. Modelling psychophysical performance

For each of eight mechanism sizes ( $\sigma_f = [1.50, 1.79, 2.08, 2.67, 3.25, 3.83, 4.42, \text{ and } 5.00]$  pixels) and for each of four stimulus weights (0.80, 1.09, 1.47, and 2.00), 200 model responses were computed for the three types of signal displays, and 200 responses were computed for null displays. In other words, there were 8 (mechanism sizes)  $\times$  4 (stimulus weights)  $\times$  3 (display types)  $\times$  2 (stimulus types; stimulus vs. null) = 192 conditions in the analysis and  $192 \times 200 = 38,400$  model responses in total. The means and variances of the 200 responses within each of the 192 conditions were then computed. (Histograms showed the response distributions to be generally normal.)

The model of Rubenstein and Sagi (1990) provides a convenient way to relate mechanism responses to performance in a 4AFC task as used here. As mentioned, the task required discriminating a signal stimulus (e.g., left obliques embedded in right obliques) from a region containing only right obliques. The principles of signal detection theory (Green & Swets, 1966) were used to calculate the probability of a correct detection for each condition based on the distribution of responses to the signal and null displays.

Eq. (1) describes the standard model of performance in an NAFC task:

$$p_c = \int_{-\infty}^{\infty} p_{\text{signal}}(x) P_{\text{null}}(x)^{N-1} dx. \quad (1)$$

In Eq. (1),  $p_{\text{signal}}(x)$  is the probability density function describing the responses of the model to the signal display (for a given model size, stimulus and mask), and  $P_{\text{null}}(x)$  is the distribution function describing the model response to the null display (for a given model size, stimulus and mask). These distributions were assumed to be normal with means and standard deviations corresponding to those yielded by the model ( $\mu_{\text{signal}}, \sigma_{\text{signal}}^2, \mu_{\text{null}}, \sigma_{\text{null}}^2$ ). We used a single free parameter ( $\sigma_{\text{noise}}$ ) to bring the model performance into the range found in the experiment. Consequently,  $p_{\text{signal}}(x)$  is a normal distribution with a mean  $\mu_{\text{signal}}$  and variance ( $\sigma_{\text{signal}}^2 + \sigma_{\text{noise}}^2$ ), and,  $P_{\text{null}}(x)$  is a cumulative normal distribution with a mean  $\mu_{\text{null}}$  and variance ( $\sigma_{\text{null}}^2 + \sigma_{\text{noise}}^2$ ). It is critical to note that the masks function only as spatial noise; there is no representation of time or temporal energy.

### 4.3. Summary of model performance

Fig. 5 summarizes the behaviour of the model. Each panel shows the proportion of correct responses for each of the three conditions (standard, noise and short) for each of eight model sizes (eccentricities). From top left to bottom right, the four panels represent *simulated* short to long SOAs; viz., stimulus weights of 0.80–2.00.

Fig. 5 may be compared with the psychophysical data in Fig. 4. It is clear that there are great similarities between the two figures, and small, but important differences. As with our psychophysical subjects, the model performance is best in the standard and noise conditions and much poorer in the short condition. As well, there is a pronounced CPD for the standard condition and no CPD for the short condition. Finally, comparing the simulated results from the standard and noise conditions reveals that the noise-mask is less effective at small scales than is the X-mask, yet at large scales the noise mask is more effective. That is, the noise mask should be less effective near fixation and more effective in the periphery, leading to a much less pronounced CPD than in the standard condition. The principle difference between the simulation and psychophysical results is that a modest CPD exists in the model response for the noise condition at the lowest stimulus weight (i.e., shortest simulated SOA), in contrast to the psychophysical results of the present experiment.

Overall, the results in Fig. 5 show show a satisfactory fit to the data. It is quite likely that the fit could be improved if the entire space of models were to be examined (e.g., by considering different first-layer filters, second-

layer filters, rectifications or size relationships between first and second layer filters) but for present purposes we wanted to understand effects of different mask and stimulus types using a more or less off-the-shelf version of the model. Clearly the noise and X-masks have different effects on performance that parallel the psychophysical data: noise is less effective at fixation and more effective in the periphery. Using the noise mask as a purely spatial source of noise affects the CPD in the same direction as predicted by the temporal theory. Therefore, failure to find a CPD with a simultaneous noise mask is not necessarily inconsistent with the spatial model (see Section 5). Finally, the short line condition is very difficult for psychophysical observers and elicits very low performance from the model; in neither case is a CPD observed.

### 5. General discussion

The psychophysical results and the results of the computational model put us in a position to address the question of whether backward masking per se is responsible for the CPD in the classic studies of [Kehrer \(1987, 1989\)](#). On balance we find little support for this proposal. Our empirical results show a strong CPD in the standard condition, a greatly attenuated or non-existent CPD in the noise mask condition and no CPD in the short-line condition, in spite of there being a backward mask in all cases. Therefore, a backward mask does not lead inevitably a CPD. To the extent that there is a modest CPD in the noise mask condition, an generic FRF model shows this effect to be an expected from the standard spatial account. Because the FRF model and the temporal theory predict an attenuated CPD when a noise mask limits performance, simultaneous masking with a noise mask ([Morikawa, 2000](#)) cannot be used to assess the contribution of temporal factors to the CPD.

On the other hand, the few cases in which absolutely no CPD is found for the noise mask condition (i.e., [Morikawa \(2000\)](#) and the shortest SOA in the present study) seems inconsistent with the standard spatial theory ([Gurnsey et al., 1996](#)) and might require elaboration of the spatial model. It should be noted, however, that because the spatial theory predicts a reduced—if not non-existent—CPD in the presence of a noise mask, one could easily interpret the absence of a CPD as a straightforward consequence of sampling error; when there is a small effect, inherent variability in subjects' responses may obscure it.

An alternative explanation for the absence of a CPD (Fig. 4, top left) is that there are different routes to solving the task. The analysis summarized in Fig. 5 assumes that the only route to discrimination is through the FRF model. Although this model seems to explain most of

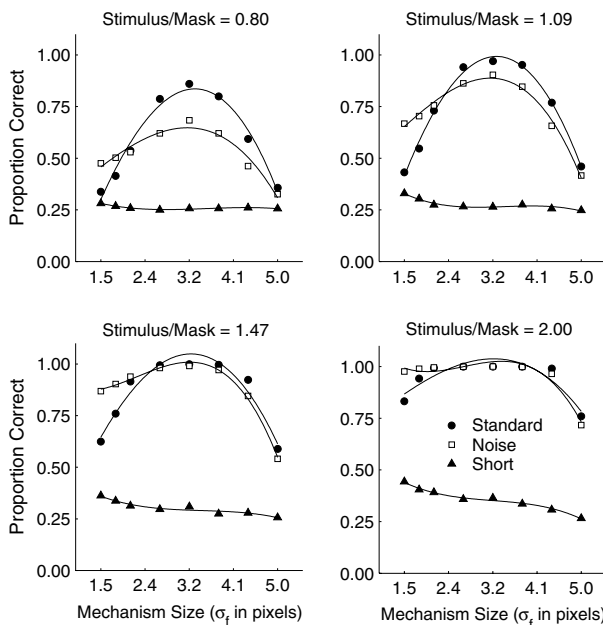


Fig. 5. Each panel shows the simulated condition by eccentricity interaction for a different *simulated* SOA.



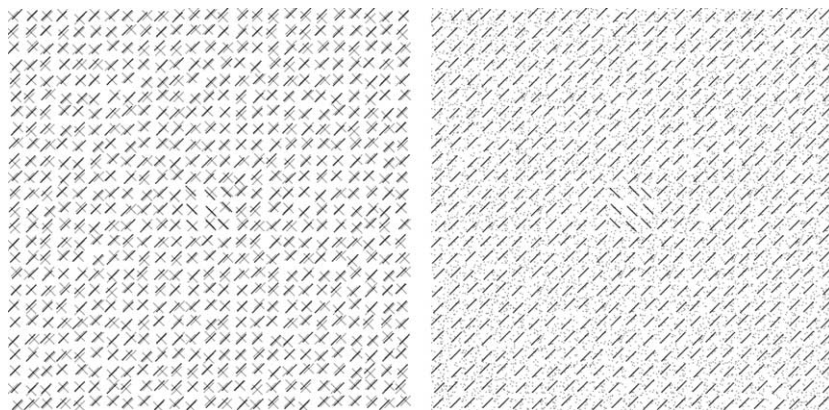


Fig. 6. It is very difficult to perceive the disparate region in the left panel when fixating its centre, whereas it is easy to see the disparate region in the right panel when fixating its centre. However, if one fixates somewhere between the right an left panels, it becomes easier to detect the disparate region in the left panel.

the variability in the psychophysical data, it is also possible that other mechanisms contribute to performance. Rather than relying on the output of an FRF model, subjects might also attempt to search item by item through the display to locate regions of discontinuity. Given our obvious ability to do this (see any number of papers in visual search; e.g., Treisman & Gelade, 1980) subjects would certainly make use of such a strategy in order to maximize performance. Our analysis of the FRF model response to the noise- and X-masks showed that the noise mask less effectively masked the texture boundary at small model scales (i.e., near fixation). This suggests that a search strategy should be more successful near fixation when the stimulus is masked by a noise mask (presented as either a backward mask or a simultaneous mask) than when the stimulus is masked by an X-mask.

Fig. 6 provides an illustration of this idea. Both left and right panels contain the same signal display. In the left panel an X-mask has been *added* to the signal and in the right panel a noise-mask has been added. Clearly, the disparate region is easier to see when fixating the centre of the right panel than when fixating the centre of the left panel. This demonstrates that the X-mask more effectively masks orientation structure than the noise-mask. However, most people find that when they move their gaze from the centre of the left panel towards the right, at some point the disparate region in the left panel becomes apparent. This illustrates the standard CPD when a simultaneous X-mask is used. Conversely, the disparate region on the right that is easily seen when fixated, becomes progressively more difficult to see when gaze is moved to the left. This illustrates the failure of the CPD in the case of a simultaneous noise mask.

A similar argument may apply to the findings in the short-line condition. Our analysis showed that under the conditions of our experiment performance in the

short-line condition should be very low and little if any CPD should be seen (consistent with the psychophysical results). Performance in the short-line condition in Morikawa (2000) was somewhat better than in the present study, yet participants only achieved 75% correct responses at an exposure duration of 106 ms with no mask. For longer lines (e.g., Fig. 1, top left) this would have produced a ceiling effect. It is quite easy to understand why such stimuli do not produce a CPD with or without a mask. If one fixates the disparate region in Fig. 1 bottom left, the texture difference is readily seen. As one fixates away from the disparate region the texture difference becomes increasingly difficult to see. Therefore, resolution loss would naturally move the performance peak closer to fixation. In addition, reducing the length of the lines increases the relative separation between them and this is well known to make discrimination more difficult (Nothdurft, 1985) and perhaps lead subjects to search element by element through the display to locate the target region. Therefore, if subjects use a search strategy to accomplish the task in the short condition, one might well expect the normal eccentricity effect rather than the CPD (e.g., Carrasco & Frieder, 1997).

In summary, we find no evidence to suggest that backward masking per se causes the CPD in the classic studies of Kehrner (1987, 1989) or in later studies by Gurnsey et al. (1996), Joffe and Scialfa (1995), Morikawa (2000), Yeshurun and Carrasco (1998, 2000) or Talgar and Carrasco (2002). This is not to say that we can categorically reject a role for temporal factors, rather, we conclude that no evidence to date is inconsistent with the simple spatial account.

#### Acknowledgments

This research was supported by NSERC and FCAR Research Grants to Rick Gurnsey.

## References

- Carrasco, M., & Frieder, K. S. (1997). Cortical magnification neutralizes the eccentricity effect in visual search. *Vision Research*, 37, 63–82.
- Green, D. M., & Swets, J. A. (1966). *Signal detection theory*. New York: John Wiley and Sons.
- Gurnsey, R., & Browse, R. (1989). Asymmetries in visual texture discrimination. *Spatial Vision*, 4, 31–44.
- Gurnsey, R., Pearson, P., & Day, D. (1996). Texture segmentation along the horizontal meridian: Nonmonotonic changes in performance with eccentricity. *Journal of Experimental Psychology: Human Perception and Performance*, 22, 738–757.
- Gurnsey, R., & Poirier, F. J. A. M. (2003). Non-monotonic eccentricity effects explained by multiple scaling theory. *Journal of Vision*, 3(9), 359a.
- Joffe, K. M., & Scialfa, C. T. (1995). Texture segmentation as a function of eccentricity, spatial frequency and target size. *Spatial Vision*, 9, 325–342.
- Kehrer, L. (1987). Perceptual segregation and retinal position. *Spatial Vision*, 2, 247–261.
- Kehrer, L. (1989). Central performance drop on perceptual segregation tasks. *Spatial Vision*, 4, 45–62.
- Kehrer, L. (1997). The central performance drop in texture segmentation: a simulation based on a spatial filter model. *Biological Cybernetics*, 77, 297–305.
- Kehrer, L., & Meinecke, C. (2003). A space-variant filter model of texture segregation: Parameter adjustment guided by psychophysical data. *Biological Cybernetics*, 88, 183–200.
- Malik, J., & Perona, P. (1990). Preattentive texture discrimination with early vision mechanisms. *Journal of the Optical Society of America A*, 7, 923–932.
- Meinecke, C. (1989). Retinal eccentricity and the detection of targets. *Psychological Research*, 51, 107–116.
- Meinecke, C., & Donk, M. (2002). Detection performance in pop-out tasks: Nonmonotonic changes with display size and eccentricity. *Perception*, 31, 591–602.
- Meinecke, C., & Kehrer, L. (1994). Peripheral and foveal segmentation of angle textures. *Perception & Psychophysics*, 56, 326–334.
- Morikawa, K. (2000). Central performance drop in texture segmentation: The role of spatial and temporal factors. *Vision Research*, 40, 3517–3526.
- Nothdurft, H. C. (1985). Orientation sensitivity and texture segmentation in patterns with different line orientation. *Vision Research*, 25, 551–560.
- Poirier, F. J. A. M., & Gurnsey, R. (2002). Two eccentricity dependent limitations on subjective contour discrimination. *Vision Research*, 42, 227–238.
- Potechin, C., & Gurnsey, R. (2003). Backward masking is not required to elicit the central performance drop. *Spatial Vision*, 16, 393–406.
- Rubenstein, B. S., & Sagi, D. (1990). Spatial variability as a limiting factor in texture-discrimination tasks: Implications for performance asymmetries. *Journal of the Optical Society of America A*, 7(9), 1632–1643.
- Treisman, A. M., & Gelade, G. (1980). A feature-integration theory of attention. *Cognitive Psychology*, 12, 97–136.
- Talgar, C. P., & Carrasco, M. (2002). Vertical meridian asymmetry in spatial resolution: Visual and attentional factors. *Psychonomic Bulletin and Review*, 9, 714–722.
- von Berg, J., Ziebell, O., & Stiehl, S. H. (2002). Texture segmentation performance related to cortical geometry. *Vision Research*, 42, 1917–1929.
- Wilson, H. R., Levi, D., Maffei, L., Rovamo, J., & De Valois, R. (1990). The perception of form: Retina to striate cortex. In L. Spillman, & J. S. Werner (Eds.), *Visual perception: The neurophysiological foundations*. New York: Academic Press.
- Yeshurun, Y., & Carrasco, M. (1998). Attention improves or impairs visual performance by enhancing spatial resolution. *Nature*, 396, 72–75.
- Yeshurun, Y., & Carrasco, M. (2000). The locus of attentional effects in texture segmentation. *Nature Neuroscience*, 3, 622–627.
- Young, R. A. (1985). *The Gaussian derivative theory of spatial vision: Analysis of cortical cell receptive field line-weighting profiles*. General Motors Research Technical Report GMR-4920.